Bull. Mater. Sci. (2023) 46:104
https://doi.org/10.1007/s12034-023-02947-x

Characterization of Ti4Al4Mo/SiC composite produced by pressure-assisted sintering

R YAMANOGLU[1,*], A BAHADOR[2], K KONDOH[3], C DURAN[1], Y AKYILDIZ[1,4], Y OZDEMIR[5] and O OZTURK[4]

[1]Engineering Faculty, Metallurgical and Materials Engineering Department, Kocaeli University, 41001 Kocaeli, Turkey
[2]Razak Faculty of Technology and Informatics, Universiti Teknologi Malaysia, 54100 Kuala Lumpur, Malaysia
[3]JWRI, Osaka University, Osaka 567-0047, Japan
[4]Onatus Vision Technologies, Gebze Organized Industrial Zone, 41400 Kocaeli, Turkey
[5]Yalova Vocational School, Yalova University, Safran Campus, Yalova 77100, Turkey
*Author for correspondence (ryamanoglu@gmail.com)

MS received 15 May 2022; accepted 30 January 2023

Abstract. In this study, a SiC-reinforced Ti4Al4Mo alloy matrix composite was designed, and produced by pressure-assisted sintering technique. Ti-4Al-4Mo (wt%) alloy was prepared from elemental powders, and different fractions of SiC (1, 5 and 10 wt%) ceramic reinforcements were homogenously distributed in the matrix by mechanical mixing and the mixtures were consolidated under 45 MPa pressure and sintered at 950°C for 10 min. Microstructure of Ti alloy matrix was studied and correlated with the CALPHAD approach. Results showed that 10 wt% SiC content caused an agglomeration of reinforcement particles and affected the properties negatively. However, hardness of the composites increased with increase in SiC content, and excellent wear properties were obtained at 1 and 5 wt% SiC content. Further increase in SiC content lead to a decrease in bending and wear properties. This study provides a new Ti4Al4Mo metal–matrix composite reinforced with SiC particles.

Keywords. Ti4Al4Mo; composite; SiC; wear; powder metallurgy.

1. Introduction

Titanium and its alloys are widely preferred in many applications such as aerospace, defence, medical and automotive due to their high specific strength and excellent corrosion resistance. Despite the excellent properties of titanium alloys, weak tribological properties limit their successful implementation in the intended applications [1, 2]. Titanium-based materials with particle reinforcements provide improved strength, excellent wear resistance and high-temperature durability. For this, titanium matrix composites attract more attention in aerospace, chemical, automotive and biomedical applications [3]. Using fine particles instead of fibre-type reinforcements supplies more isotropic properties and relative ease of production. Besides, fibre-reinforced composites are economically unattractive for large volume productions [4, 5]. Even small amounts of ceramic particles can enhance the tribological properties of the titanium matrix composites [6, 7]. Different type of ceramic reinforcements, including TiC [8], TiB [9], TiB_2 [10], B_4C [11], ZrO_2 [12], Al_2O_3 [13], TiN [14], Si_3N_4 [6], SiC [15], have been reported for the titanium metal–matrix composites.

These reinforcements are generally introduced with the metal matrix by *ex-situ* methods using stir casting, spray forming or powder metallurgy (PM). The final properties of the composite materials strongly depend on the homogenous distribution of ceramic phases in the metal matrix material and the interfacial coherence between the matrix and the second-phase reinforcements [16]. It is expected that the hardness, wear and strength of the matrix material increase with increasing ceramic-reinforcement content. However, a high amount of the second phase can cause agglomeration, and their homogenous distribution in the matrix becomes difficult. To overcome these difficulties, PM has many advantages for a homogenous distribution of the reinforcing particles with metal particles even if using low-energy ball milling routes. Besides, solid-state sintering by PM produces strong bonding of the compounds for a load transfer at the interface [17, 18]. Therefore, PM is one of the most preferred production techniques for the fabrication of ceramic particle-reinforced titanium matrix composites. PM also provides near-net-shape processing of the materials, minimal material waste and microstructural control [19, 20].

The microstructure of titanium-based materials significantly affects their final properties [21]. The microstructure of titanium alloys is controlled by their phases. Ti shows an allotropic phase transition from hcp (α) to bcc (β) at 882°C.

Published online: 19 May 2023

Therefore, α, β and α + β phases are generally seen in the microstructure [22, 23]. Pure titanium (α) and Ti6Al4V alloy (α + β) are used in most industrial applications [24, 25]. However, recently, the need for different titanium-based materials has increased with technological developments. Mostly molybdenum (Mo)-containing compositions are preferred in the design of new titanium alloys [26]. Besides, V in Ti6Al4V makes this alloy expensive. If titanium is alloyed with Mo instead of V, the raw material costs are lowered. Yan *et al* [27] studied Ti-4.5Al-6.8Mo-1.5Fe (wt%) alloy, and they stated that compared to the Ti6Al4V alloy if the material consists of Fe and Mo instead of V, the cost of the material can be lowered up to 30% [27]. Mo and Al affect the crystal structure of Ti as β- and α-stabilizers, respectively, and present a modified microstructure [28, 29]. The addition of Mo also improves the corrosion properties of titanium alloys [30–33].

In this study, Ti4Al4Mo alloy was selected as a metal matrix, and a new composite was developed for use in industrial applications by reinforcing the effect of SiC particles. Powder metallurgical processes have been preferred for composite production, and superior properties have been achieved.

2. Experimental

The commercially pure Ti (ASTM Grade 2), Al, Mo and SiC powders were used to fabricate Ti4Al4Mo-*x*SiC composites (x = 1, 5 and 10 wt%). The scanning electron microscopy (SEM) images of the powders used in this study are given in figure 1. Powders were mixed in a zirconia jar using zirconia balls (5 mm in diameter) under a vacuum environment (10^{-4} mbar) at 330 rpm rotation speed and 30 min rotation cycle with a 15 min gap. Three different mixing steps were applied to the mixtures due to the different melting temperatures, particle sizes and density properties of each alloying element. These steps were determined according to our previous experiments for a homogenous distribution of the constituents. The mixing steps showing the mixing times are given in table 1. First, Ti and Mo powders were mixed in the zirconia jar for 30 min. Then Al powders were added to obtain Ti4Al4Mo composition. The mixing process was maintained for a further 120 min. Finally, the SiC powders were added to the mixture and stirred for further 60 min. Therefore, the total composite mixture preparation cycle lasted 210 min.

The premixed powders were consolidated using uniaxial pressure-assisted sintering (DIEX VS 50). A three-stage sintering cycle, as shown in figure 2, was used for the composite fabrication process. Melting temperatures of the components were taken into consideration in determining the sintering steps. Low melting materials are generally used without any problems in conventional powder metallurgical processes as in liquid phase sintering methods. However, in our study, since a pressure-assisted process was chosen for composite production, it was necessary to use such gradual temperature cycles to keep the liquid phases under pressure without leaving the graphite die. For this reason, 10 min holding time is determined at 500 and 780°C for adequate diffusion of Al in the system, and then the temperature was increased to 950°C for the final step of sintering for all components. The pressure value of 45 MPa was kept constant throughout the whole process. The non-reinforced Ti4Al4Mo sample was also produced with a similar process as the reference material. A 10^{-4} mbar vacuum atmosphere was used during the sintering process to prevent oxidation of the samples. An image of the graphite die kept at 950°C during experiment is shown in figure 2.

Densities of as-produced composites were evaluated from Archimedes method. Thereafter, samples were ground (up to 2000 grit size), polished (using diamond solution; 9, 6 and 3 μm particles) and etched (etchant: HF:HCl:H_2O (3:6:91)). The Vickers hardness test was conducted using a Future Tech Vickers Hardness tester using 10 kg force for 10 s dwell time. The samples were then cut to the size of 4 × 4 × 20 mm, and ground for the three-point bending test. Dry sliding wear tests were conducted in the Turkyus POD&TTW ball-on-disc type wear test device following ASTM G99-05 standards. Wear tests were carried out at room temperature under 20 N load using AISI 52100 steel balls (5 mm in diameter) as the counterface. The sliding distance and speed were determined as 250 m and 150 rpm, respectively, for all the tests. The samples were cleaned with alcohol and dried with a hot-air blower. Then they were weighed, and their weight losses were determined, and wear rate values were calculated according to the following formula. $W = Md^{-1}D^{-1}$, where W is the wear rate (mm^3 m^{-1}), M donates mass loss (g), and d (g mm^{-3}) and D (m) are the density and sliding distance during the wear test, respectively. The microstructural characterization and worn surface of the samples were investigated using scanning electron microscopy (JEOL JSM 6060) equipped with an energy dispersive X-ray spectrometer.

3. Results and discussion

One of the most important properties of particle-reinforced composites is density. Figure 3 shows the density values of Ti4Al4Mo alloy without and with the addition of SiC powders. Theoretical densities of Ti4Al4Mo and SiC are 4.7 and 3.21 g cm^{-3}, respectively. Density values were measured in a helium gas pycnometer. The density of the titanium matrix composites showed a gradual decrease with increase in SiC content due to the lower density of SiC powders compared to titanium alloys. The density of Ti4Al4Mo without SiC addition was measured as 4.49 g cm^{-3}. Density values for the 1, 5 and 10 wt% SiC content was recorded as 4.48, 4.44 and 4.37 g cm^{-3}, respectively. An approximately 3% decrease was observed

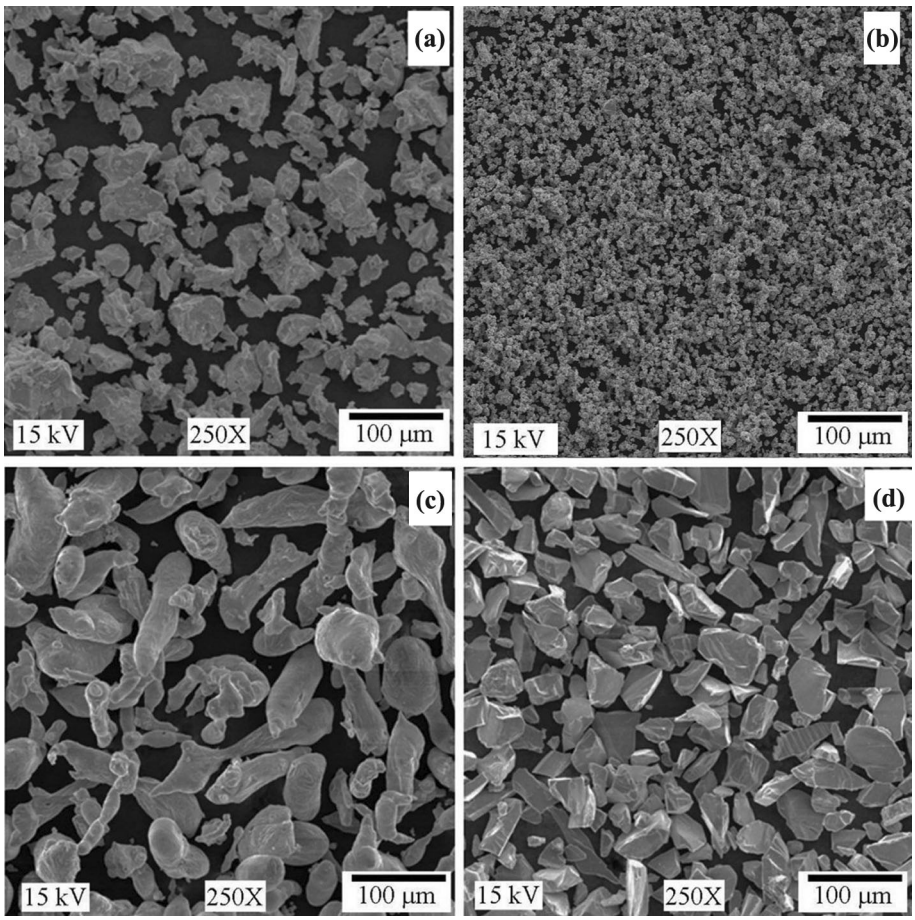

Figure 1. SEM images of powders used for composite production: (**a**) Ti, (**b**) Mo, (**c**) Al and (**d**) SiC.

Table 1. Mixing durations for Ti4Al4Mo-*x*SiC preparation.

Process stage	Composition (wt%)	Time (min)
1	*Ti-4Mo	30
2	*Ti-4Al-4Mo	120
3	*Ti-4Al-4Mo-xSiC (x = 1, 5 and 10 wt%)	60

Note: * = Balance.

for the highest content of SiC. Therefore, this result is significant for design of a new composite with lower density and higher mechanical properties for titanium alloys.

In this study, Ti4Al4Mo alloy as matrix material is fabricated from elemental powders. Homogeneous distribution of each elemental powder in the structure is essential to the final properties of the produced composite. The low melting point of Al, which is one of the alloying elements, allows it to move quickly as a liquid phase among other high melting temperature particles in the production process. The liquid phase creates an advantage both for homogenous distribution and for obtaining high density by filling the gaps between the particles. Therefore, two additional steps were added at low temperatures and held for 10 min to dissolve Al in Ti matrix. In this way, the liquid phase of Al formed during the process is prevented from coming out of the graphite die under pressure sintering. Mo has a finer particle size compared to the other particles, as can be seen in figure 1. The fine particle size of Mo powder contributes to the increase in density by filling the gaps between Ti particles. Homogenous distribution of SiC-reinforcement phase in the Ti alloy matrix was successfully achieved with a low energy ball milling process. Optical microscope and SEM images of composites with different amounts of SiC are

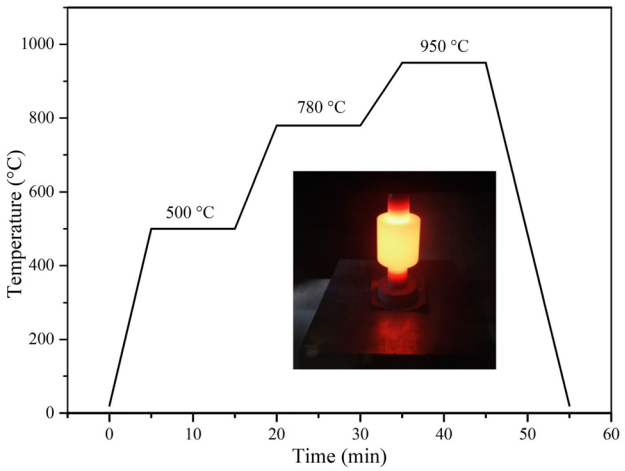

Figure 2. Sintering cycle of the Ti4Al4Mo-*x*SiC composites by hot press.

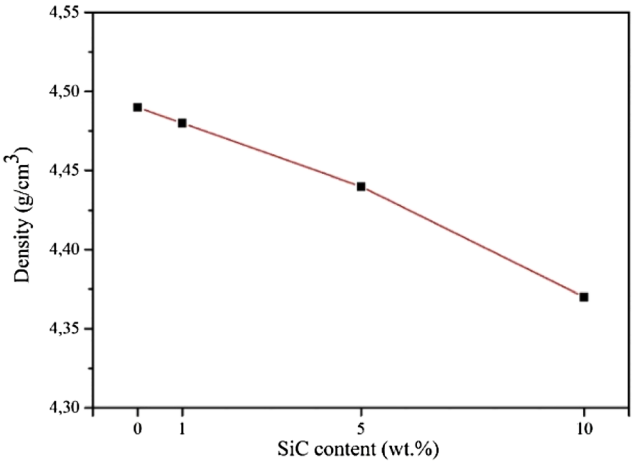

Figure 3. Density values of Ti4Al4Mo-*x*SiC composites produced by hot press.

given in figure 4. Different phases have been defined in various contrast, as can be seen from the etched microstructures. A schematic image is also provided in figure 5 for a better understanding of the phases formed during the pressure-assisted sintering of elemental powders. In titanium alloys, Al is α-stabilizer, while Mo acts as an effective β-stabilizer. In TiAlMo system, for low Al content, when Mo ratio increased to 3 wt% or higher, β-phase is dominated. Lu *et al* [34] studied Ti-6Al-*x*Mo alloys, and reported that with addition of 1 wt% Mo to Ti-6Al, the microstructure consisted mainly of α–phase. They found that the microstructure did not change with a low Mo content. However, with Mo content 3 wt% or higher, the microstructure consisted of α + β phases [34]. The striking aspect of Lu *et al*'s work is use of arc-melting vacuum casting method for material production. The α + β structure was formed even with the diffusion that took place in the liquid state where atomic mobility is relatively high. Therefore, it is necessary to reveal the effect of PM used in our study on the microstructural transformations. Contrary to casting, slow diffusion of elements is dominant in powder metallurgical processes due to the reactions taking place in solid-state [27]. Longer process times are required for sufficient atomic motion. As a result, based on elemental powder usage in our composite production process, α, β and α + β phases are generally expected to be present in the TiAlMo system (figures 4a, b and 5). Considering the dissolution of Al and Mo in titanium depending on their melting points, different regions are found at the same time depending on the sintering temperature and time. Since Al has a low melting point, it dissolved in titanium during the selected sintering temperature, and its α-stabilizing effect is seen in the microstructure. Besides, the β-phase begins to appear with the addition of Mo. β-rich regions appear at the Ti particle boundaries with a high amount of Mo in the structure. Therefore, α + β phases are clearly seen in the microstructure with the effect of Al and Mo at the same time.

Another critical point that draws attention is that the high melting point Mo does not entirely dissolve during the sintering process (figure 4a). As stated before, SiC distributions were homogeneous as the reinforcement phase in the matrix (figure 4b, c and d). It is seen that SiC powders with 10 wt% content cause an agglomeration in the structure, as indicated in figure 4d. No samples with higher SiC contents were produced due to increased agglomeration. Besides, as discussed in the next sections, this agglomeration has adversely affected the properties of composite material. In composite materials, generally, to increase the compatibility between matrix and the reinforcement phases, ceramic powders are *in-situ* formed in the matrix by chemical reactions [35]. To obtain a strong bonding between particles and matrix without any reaction or not using any chemical compound is meaningful for the composite production. In our study, the strong bonding of SiC and matrix is also remarkable. A reaction zone appeared between the SiC and the matrix. This interface is shown in the high-magnification image at the upper right in figure 4d. In composite materials, the properties are positively affected by this strong connection of the interface. The good bonding between SiC and titanium alloys was also indicated by different studies. The presence of strong bonding was correlated to the excellent wettability properties between reinforcing ceramic phases and titanium alloys [36].

Due to the use of elemental powders in TiAlMo system, since aluminium has a low melting point, it is completely dissolved, but the high melting point Mo has remained undissolved. For this reason, to better understand the interaction between Ti and Mo and its relationship with microstructure, the phase diagram and phase ratios are established by the Calphad approach (CALculation of PHAse Diagram) by Thermo-Calc software (Thermo-Calc 2020b, TCTI2) and are given in figure 6. Calphad is a useful method to determine the effect of elements on the transformation temperature [37]. Mo is a significant β-stabilizing

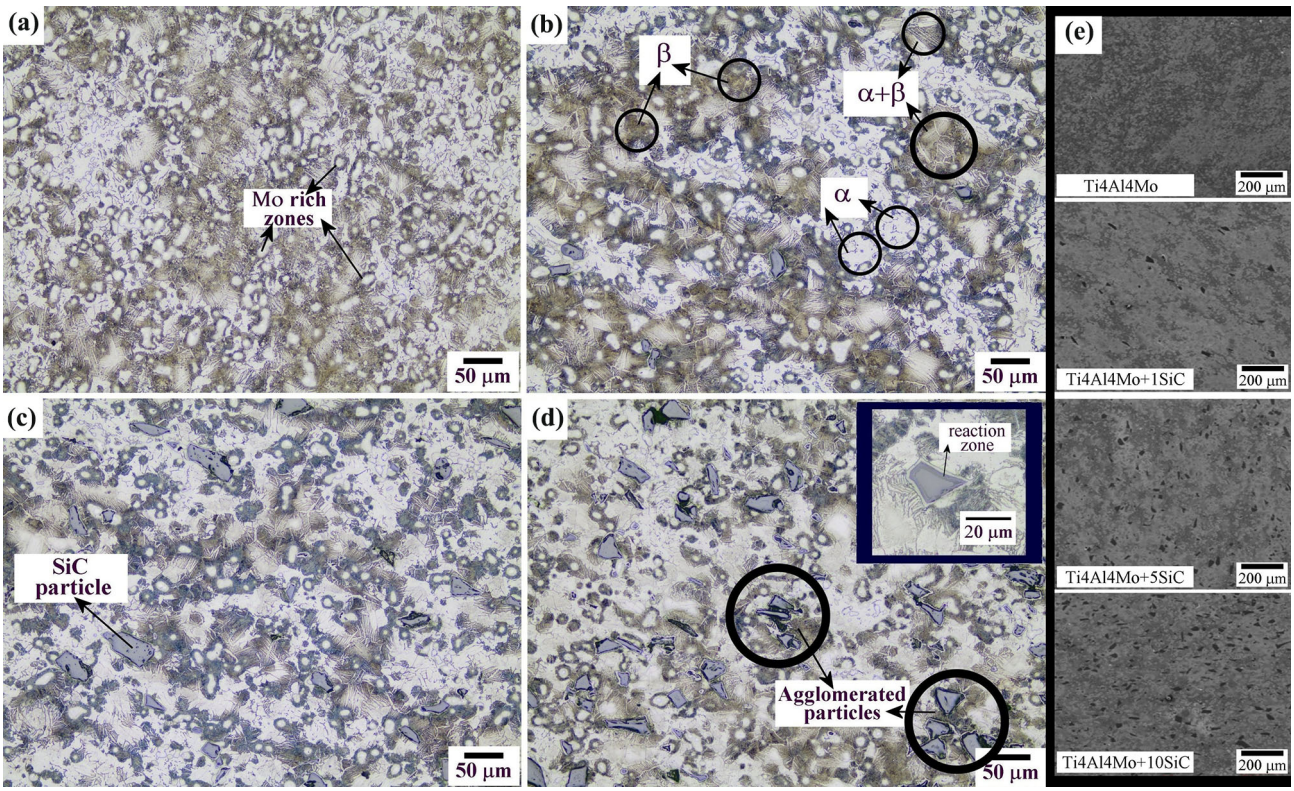

Figure 4. Optical micrographs of etched materials: (**a**)Ti4Al4Mo, (**b**) Ti4Al4Mo-1SiC, (**c**) Ti4Al4Mo-5SiC and (**d**) Ti4Al4Mo-10SiC. (**e**) SEM images of each composition showing the homogenous distribution of the SiC reinforcements.

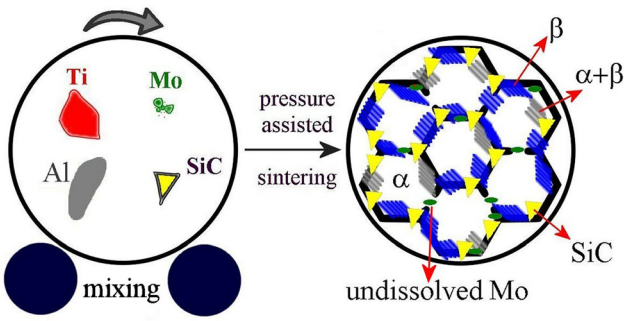

Figure 5. Schematic of microstructure after sintering of Ti4Al4Mo-SiC composite.

element. It makes the β-phase stable at low temperatures by lowering the β-transition temperature. While the transformation temperature in pure titanium is 882°C (figure 6b), this temperature is expected to decrease to lower values with Mo addition as in this study. The α + β transformation temperature for Ti-10Mo alloy is 765°C (figure 6c). However, the essential point to be considered is that, as stated before, pre-alloyed powders are not used in the study. Therefore, even if 10 wt% Mo is added to titanium, this ratio should be taken as 50 wt% at Mo and Ti particle contact points for elemental powders. With this approach, the β-transformation temperature decreases to 391°C in the calculation made by ThermoCalc software (figure 6d). It is expected that a large number of β-zones will be encountered in the titanium particle boundaries, as shown in figures 4 and 5, with the addition of a high amount of Mo. Therefore, there is a good correlation between CALPHAD methodology and experimental investigation of the microstructure, as shown in figure 6d. An illustration of this approach is presented as a thumbnail in figure 6d. Indeed, β-rich zones in the intermediate layer attract attention to the interaction of Mo and Ti particles. It is also seen that the structure of Ti particles transforms from α to α + β with the diffusion of Mo through titanium particles centres.

SEM images were also taken, and EDX analysis was performed from different points for the microstructural characterization of produced composites. Figure 7a and b shows the EDX analysed regions in the microstructure, and table 2 shows the chemical compositions of the selected points. Phases with different contrast supporting the optical microscope images draw attention in figure 7a. Mo remained undissolved since it has a high melting temperature. Undissolved Mo was shown as point 1 in figure 7a. Zone 2 represents the interaction region of both Al and Mo with titanium in the structure. Therefore, the structure consists of α + β phases as expected. Far from the Mo-rich area (point 3), there is mostly Al in Ti and, the structure consists of α. Zone 4 has a similar chemical composition to zone 3. In this zone, Al content is high, while Mo content is relatively low. Based on this approach, it can be stated that this region also consists of α-phase. Therefore, the structure

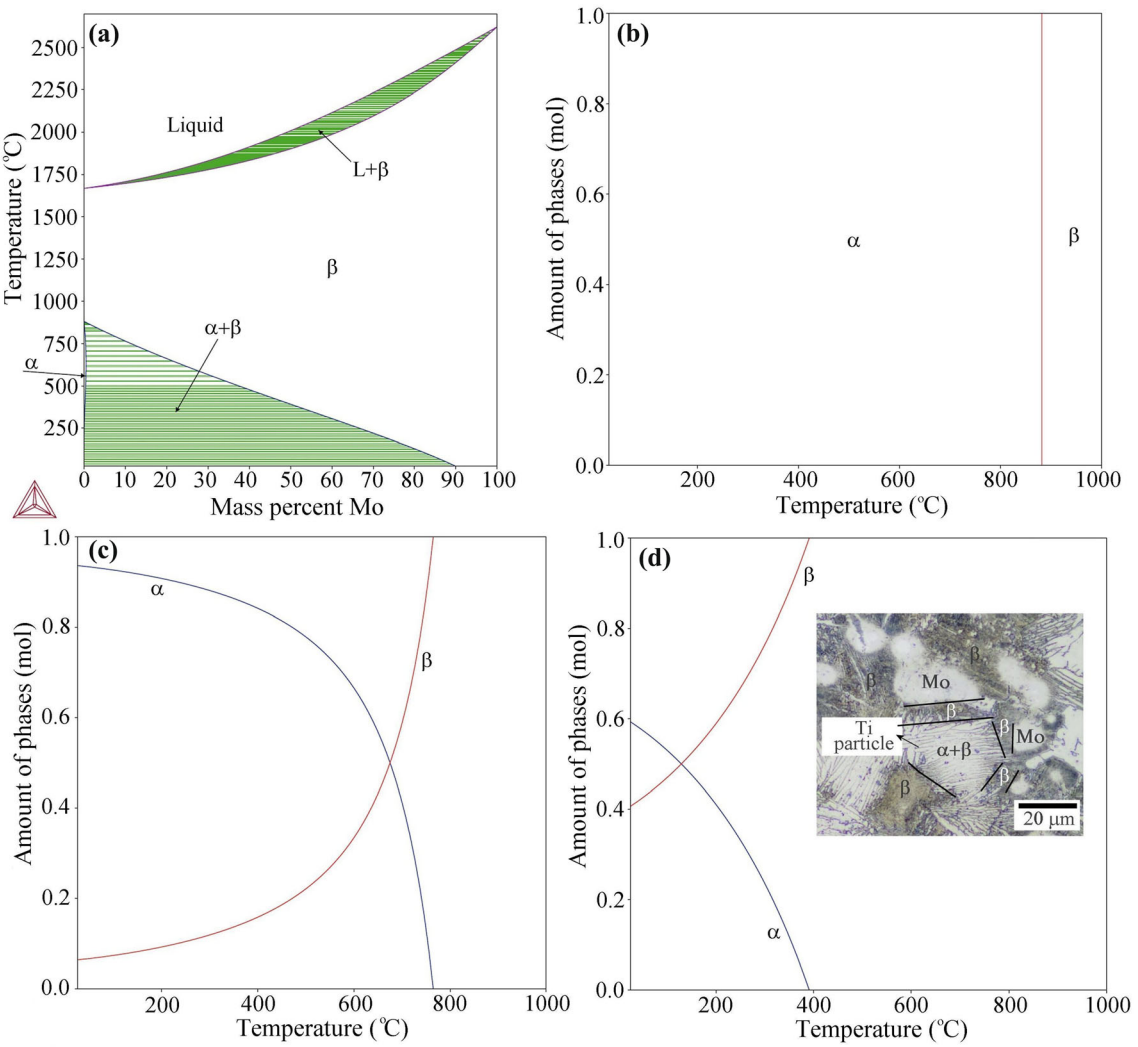

Figure 6. (**a**) Ti-Mo phase diagram, (**b**) calculated transformation temperature for pure Ti, (**c**) calculated mole fraction of phases for Ti-10Mo, and (**d**) calculated mole fraction of phases for Ti-50Mo.

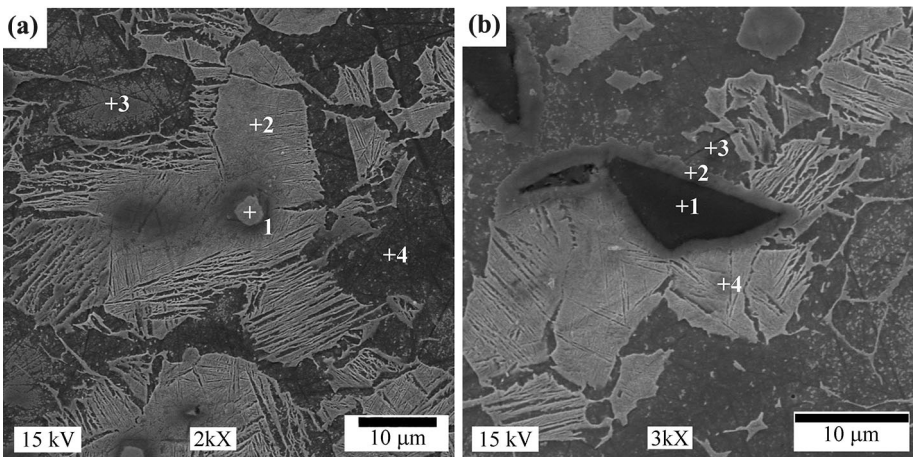

Figure 7. SEM images of (**a**) Ti4Al4Mo matrix and (**b**) interaction zones between a SiC particle and Ti alloy matrix.

Table 2. Chemical composition of different phases of Ti4Al4Mo-SiC composite.

		Composition (wt%)					
	Point	Ti	Al	Mo	Si	C	Phase
Figure 7a, Ti4Al4Mo matrix	1	1.32	—	98.68	—	—	Undissolved Mo
	2	80.56	6.80	12.64	—	—	α + β
	3	94.14	5.25	0.61	—	—	α
	4	89.00	10.11	0.89	—	—	α
Figure 7b, Ti4Al4Mo-SiC	1	—	—	—	74.29	25.71	SiC
	2	71.32	2.41	0.79	25.48	—	Interface
	3	86.63	11.31	1.25	0.81		α
	4	77.03	9.12	13.16	0.69		α + β

of Ti4Al4Mo alloy produced from elemental powders within the scope of the study has a very complex microstructure. SiC particulates were distributed homogenously in the complex structure, as shown in figure 4e. When the composite is made with a reinforcement material in a metallic matrix, especially with a ceramic character, one of the first desired properties is a strong interaction between the reinforcement phase and the matrix. Figure 7b shows a SiC particle settled in this Ti alloy matrix. It is seen that an interaction zone is formed at the contact points of the SiC particles corresponding to α + β and the only α-phase, as shown in figure 7a. Besides, no crack and pore formation was observed in these interaction regions. In table 2, EDX analysis results of the interaction regions between SiC and Ti4Al4Mo are also given. While the Al and Si content is high in interaction zone 2 (figure 7b), the Mo amount is relatively low. The strong bonding of matrix and ceramic phases affects the strength of the composites, especially in load-bearing applications. When the interaction is weak, a crack can originate at the interface and propagate among the ceramic phases and metal matrix. This weak interface causes a decrement in fracture energy. On the other hand, if the interaction is strong, the crack propagates through the ceramic phases, resulting in enhanced toughness [38]. Point 3 consists of α-phase as in regions 3 and 4, shown in figure 7a. Point 4 in figure 7b contains Al and relatively high Mo content. The phase structure in this region is defined α + β according to this composition.

Figure 8 shows the hardness test results of the SiC-reinforced Ti4Al4Mo matrix composites and the unreinforced Ti4Al4Mo alloy as a comparison. As expected, an increase was recorded in the hardness of titanium matrix composites with increase in SiC content due to the relatively higher hardness of ceramics compared to the metals. The hardness of the Ti4Al4Mo alloy without any reinforcements phase was 360 HV, as seen in figure 8, while the hardness values of 1, 5 and 10 wt% SiC content was measured as 377, 398 and 424 HV, respectively. This increase in hardness can be associated with the homogeneous distribution and micron

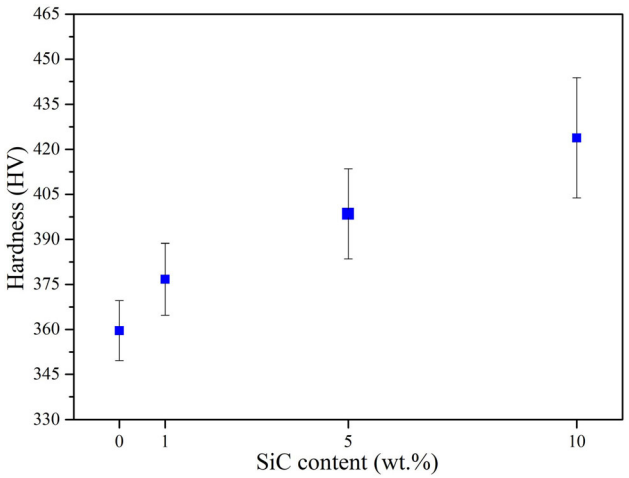

Figure 8. Hardness *vs.* SiC content.

sizes of the reinforcement phases. SiC ceramic powders are added to titanium-based materials in different sizes. Sivakumar *et al* [39] added nano-sized SiC powders to the Ti6Al4V matrix, but they reported a decrease in the hardness of the composite at high SiC contents. They attributed the decrease in hardness to the agglomeration of nano-sized SiC particles in the matrix. They demonstrated the critical effect of the porosities in the structure after the sintering process due to the high amount of agglomeration. Although the hardness of the matrix increased from 380 to 469 HV with the addition of 5 wt% nano-SiC, the hardness decreased to 369 and 315 HV, respectively at 10 and 15 wt% SiC content. Sivakumar *et al* [39] also stated that although this hardness decrease was attributed mainly to agglomeration as mentioned above, it could also be related to thermal expansion mismatch between SiC particles and matrix. An increase in the hardness of the composite material causes the brittleness of the material. For this reason, the effect of increased hardness values on the bending strength of the composite materials was also examined, and the results are given in figure 9. An increase in bending strength was observed at 1 wt% SiC content

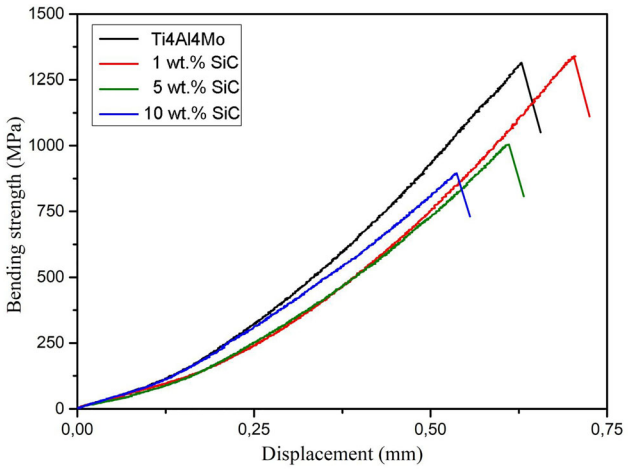

Figure 9. Bending strength of Ti4Al4Mo-*x*SiC composites.

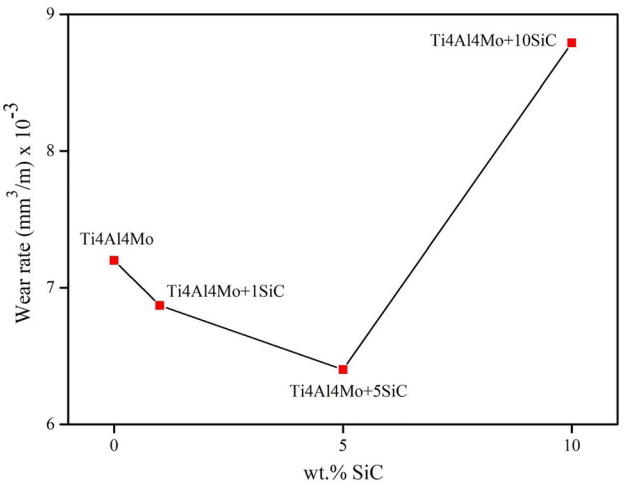

Figure 10. Wear rates of the Ti4Al4Mo-*x*SiC composites produced by hot pressing.

(1330 ± 13 MPa) compared to non-reinforced alloy (1314 ± 9 MPa). However, with increase in reinforcement phase, the bending strength was recorded as 1004 ± 16 and 895 ± 21 MPa for 5 and 10 wt% SiC contents, respectively. Increasing hardness with the effect of SiC content made the material brittle as expected, and the bending strength decreased. Similarly, the decrease in bending strength may be due to increased SiC-reinforcement content. The addition of high content of SiC causes agglomeration and prevents the material from full densification during sintering [40]. The porosities between SiC powders play an important role in strength reduction. Besides, the primary mechanism of the increase in strength with the addition of low amounts of SiC was based on the strong interaction between the SiC particle and the matrix [36]. Liu *et al* [41] also stated that there is a decrease in mechanical properties with the increase in amount of reinforcement phase ratio in composite formation with the addition of SiC. In their study, titanium was reinforced with SiC nanowires, and a decrease in mechanical properties was observed after 5 wt% reinforcement content [41].

Although pure titanium and titanium alloys have many advantages, one of the essential points limiting their use in industrial applications is their weak wear resistance. An *ex-situ* process is formed, and no new compounds appeared between the Ti matrix and reinforcements during sintering by addition of the SiC powders to the matrix by low energy ball milling. For these reasons, in the formation of composites with titanium matrix, the addition of thermodynamically stable ceramic powders such as SiC and the densification of this mixture through sintering enhanced developments in wear resistance is expected [42]. In this study, dry sliding wear tests of SiC-reinforced TiAl4Mo matrix composite was performed at room temperature, and the wear rates obtained after wear tests are given in figure 10. Except for 10 wt% SiC content, the wear resistance was increased compared to the TiAl4Mo alloy and thus, wear rates were decreased with increase in SiC content. The highest wear resistance was determined at 5 wt% SiC content. For the 10 wt% SiC content, the wear properties of the composite were negatively affected, and the wear rate increased effectively. The improvement in wear behaviour is attributed to the increased hardness of the material with SiC reinforcements. Harder ceramic phases improve the wear resistance of the softer metal matrix. Harder materials show higher wear resistance, according to Archard's law. As more SiC powders are introduced to the titanium matrix, the hardness of the composite increases, as shown in figure 8, and wear resistance increases. Archard's law proves this approach based on the wear volume V, load F, sliding distance D and hardness HV as follows: $V = cDF/3HV$, where c is a dimensionless wear constant [38]. The negative effect of wear properties at 10 wt% SiC content is related to the agglomeration of the ceramic powders. Decreased wear rate is associated with the reinforcing phases removed from the matrix under dry sliding conditions, causing an increase in weight loss. It is thought that the Mo content in the structure is as effective as the reinforcement phases in the development of the wear properties of the produced composite. One of the most important reasons underlying the wear properties of Ti alloys is the oxide layer that is poorly bonded to the surface. The superior corrosion resistance achieved by the oxide layer formed by Mo on the surface of the materials is influential in providing an enhanced wear behaviour of titanium compared to its oxides [43]. Therefore, even the matrix material produced from elemental powder will be attractive for the titanium industry in applications where wear properties should be prioritized.

The SEM images of the worn surfaces also support the wear rate results (figure 11). In figure 11a–d, the wear trace widths are revealed with the addition of SiC. In figure 11e, a high-magnification view of the sample with the highest SiC content is also given. As a result of the surface examination, it is stated that the reduction in wear track widths is

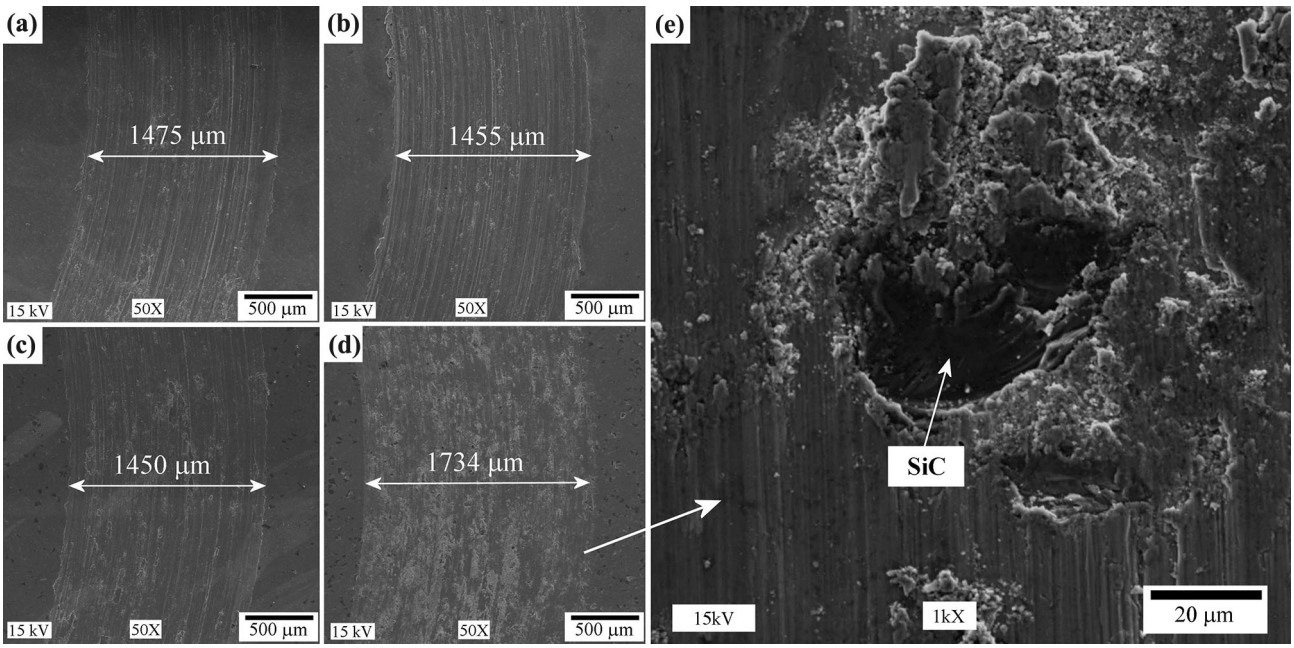

Figure 11. SEM images of the worn surfaces: (**a**) Ti4Al4Mo, (**b**) Ti4Al4Mo+1SiC, (**c**) Ti4Al4Mo+5SiC and (**d**) Ti4Al4Mo+10SiC. (**e**) High-magnification image of the composite with highest SiC content.

remarkable with SiC addition. Although the wear trace widths of the composites containing 1 and 5 wt% SiC are close to each other, they remained below compared to the Ti4Al4Mo alloy matrix. In the composite containing 10 wt% SiC, it is seen that the wear trace width increased considerably. In Ti4Al4Mo and composites with 1–5 wt% SiC content, the main wear mechanisms are abrasive, adhesive and delamination. In contrast, in the highest SiC content, the wear mechanism is predominantly delamination. The worn surfaces of the composites tend to be smoother, with shallow grooves indicating an abrasive wear mechanism. Similar to wear rate results, Ti4Al4Mo-10SiC composite has the highest wear track than other all samples. The main reason for the higher wear rate and the widest worn track in TiAl4AMo+10SiC is due to the high amount of agglomerated SiC content. As indicated in figure 11e, the matrix material was easily peeled off from the surfaces, and an intense delamination wear mechanism was revealed.

4. Conclusion

Metal–matrix composite compositions are produced every day to meet the expectations in industrial applications. In this study, a Ti4Al4Mo alloy matrix composite reinforced with SiC powders was successfully produced. The following results are obtained:

1. Elemental powders are mixed homogenously in a ball mill and consolidated by a vacuum hot press. Although Al has a low melting point, it was kept inside the structure without leaving the graphite die during pressure-assisted sintering.
2. Three different SiC contents (1, 5 and 10 wt%) were used for the composite fabrication. At 10 wt% SiC content, the reinforcement phases started to agglomerate and negatively affected some properties. However, the hardness of the Ti4Al4Mo matrix composite increased with increasing SiC content. The hardness of the non-reinforced material was 360 HV, while the hardness of the composite containing 10 wt% SiC increased to 424 HV.
3. The low amount of SiC content made a positive contribution to the bending strength of the composite. The bending strength of 1 wt% SiC composite increased from 1314 to 1330 MPa compared to non-reinforced Ti4Al4Mo alloy. However, the increased SiC content showed a negative effect on the bending strength, and it decreased up to 895 MPa at the highest SiC content.
4. The most important results of the study were obtained in wear properties. As a function of an increase in hardness with increasing SiC content, wear resistance improved and wear rate decreased. However, due to agglomeration caused by the increased SiC content, an adverse effect was seen on the wear properties at 10 wt% SiC content, and the wear rate increased.

The superior properties obtained in this study were associated with the homogenous reinforcement distribution and strong interaction between the matrix and ceramic phases by PM. Although there is a negative effect on the properties with the increasing reinforcement phase ratio, within the scope of this study, a new and unique titanium

metal–matrix composite with 5 wt% SiC content with high hardness and enhanced wear properties was designed and brought to the literature.

Acknowledgement

This study was supported by the Scientific Research Project Unit of Kocaeli University (Grant Number 2018/158).

References

[1] Koo M Y, Park J S, Park M K, Kim K T and Hong S H 2012 *Scr. Mater.* **66** 487
[2] Katsuyoshi K, Ryuho I, Junko U, Shota K and Khantachawana A 2019 *Mater. Sci. Eng. A* **739** 491
[3] Duan H, Han Y, Lu W, Wang L, Mao J and Zhang D 2016 *Mater. Des.* **99** 219
[4] Hayat M D, Singh H, Miodowski A, Bokhari S W, He Z and Cao P 2020 *Int. J. Refract. Met. Hard. Mater.* **92** 105257
[5] Bahador A, Umeda J, Yamanoglu R, Ghandvar H, Issariyapat A, Abu Bakar T A *et al* 2020 *J. Alloys Compd.* **847** 156555
[6] Singh H, Hayat M D, Zhang H and Cao P 2019 *Wear* **420–421** 87
[7] Poletti C, Balog M, Schubert T, Liedtke V and Edtmaier C 2008 Compos. *Sci Technol.* **68** 2171
[8] Gu D, Wang Z, Shen Y, Li Q and Li Y 2009 *Appl. Surf. Sci.* **255** 9230
[9] Singh H, Hayat M, He Z, Peterson V K, Das R and Cao P 2019 *Compos. Part A Appl. Sci. Manuf.* **124** 105501
[10] Hu C L and Sun R L 2020 *IOP Conf. Ser. Mater. Sci. Eng.* **770** 012003
[11] Ota A, Egawa H and Izui H 2012 *Mater. Sci. Forum.* **706–709** 222
[12] Abd-Elwahed M S, Ibrahim A F and Reda M M 2020 *J. Mater. Res. Technol.* **9** 8528
[13] Shi S, Cho S, Goto T and Sekino T 2020 *Mater. Today Commun.* **25** 101522
[14] Zhou S, Zhao Y, Wang X, Li W, Chen D and Sercombe T B 2020 *J. Alloys Compd.* **820** 153422
[15] Lobley C M and Guo Z X 2013 *Mater. Sci. Technol.* **14** 1024
[16] Shehata F, Fathy A, Abdelhameed M and Moustafa S F 2009 *Mater. Des.* **30** 2756
[17] Kondoh K, Biao C and Umeda J 2019 *Powder Metallurgy Processes for Composite–Materials Integration* In: Setsuhara, Y, Kamiya T, Yamaura Si (eds) *Novel Structured Metallic and Inorganic Materials* (Singapore: Springer) https://doi.org/10.1007/978-981-13-7611-5_16
[18] Yamanoglu R, Zeren M and German R 2012 *J. Min. Metall. B* **48** 73
[19] Morsi K 2019 *J. Mater. Sci.* **54** 6753
[20] Yamanoglu R 2019 *Powder Metall. Met. Ceram.* **57** 513
[21] Fidan S, Avcu E, Karakulak E, Yamanoglu R, Zeren M and Sinmazcelik T 2013 *Mater. Sci. Technol.* **29** 1088
[22] Chen W, Li C, Zhang X, Chen C, Lin Y C and Zhou K 2019 *J. Alloys Compd.* **783** 709
[23] Yamanoglu R, German R M, Karagoz S, Bradbury W L, Zeren M, Li W *et al* 2013 *Powder Metall.* **54** 604
[24] Ongtrakulkij G, Khantachawana A and Kondoh K 2020 *Surf. Interfaces* **18** 100424
[25] Yamanoglu R, Efendi E, Kolayli F, Uzuner H and Daoud I 2018 *Biomed. Mater.* **13** 025013
[26] Kolli R and Devaraj A 2018 *Metals* **8** 506
[27] Yan Z, Chen F, Cai Y and Zheng Y 2014 *Powder Technol.* **267** 309
[28] Yamanoglu R, Bahador A and Kondoh K 2021 *J. Mater. Eng. Perform.* **30** 3203
[29] Fidan S, Avcu E, Karakulak E, Yamanoglu R, Zeren M and Sinmazcelik T 2013 *Mater. Sci. Technol.* **29** 1088
[30] Zhou Y-L and Luo D-M 2011 *J. Alloys Compd.* **509** 6267
[31] Tarzimoghadam Z, Sandlöbes S, Pradeep K G and Raabe D 2015 *Acta Mater.* **97** 291
[32] Oliveira N T C, Aleixo G, Caram R and Guastaldi A C 2007 *Mater. Sci. Eng. A* **452–453** 727
[33] Yamanoglu R 2021 *Met. Powder Rep.* **76** 32
[34] Lu J W, Ge P, Zhao Y Q and Niu H Z 2013 *Mater. Sci. Eng. A* **584** 41
[35] Guo X, Wang L, Wang M, Qin J, Zhang D and Lu W 2012 *Acta Mater.* **60** 2656
[36] Falodun O E, Obadele B A, Oke S R, Okoro A M and Olubambi P A 2019 *Int. J. Adv. Manuf. Technol.* **102** 1689
[37] Degnah A, Du J and Ravi Chandran K S 2020 *Mater. Sci. Eng. A* **781** 139210
[38] German R M 2016 *Particulate composites fundamentals and applications* (Switzerland: Springer)
[39] Sivakumar G, Ananthi V and Ramanathan S 2017 *Trans. Nonferrous Met. Soc. China* **27** 82
[40] Falodun O E, Obadele B A, Oke S R, Ige O O, Olubambi P A, Lethabane M L *et al* 2018 *Trans. Nonferrous Met. Soc. China* **28** 47
[41] Liu Y, Dong L, Lu J, Huo W, Du Y, Zhang W *et al* 2020 *J. Alloys Compd.* **819** 152953
[42] Hayat M D, Singh H, He Z and Cao P 2019 *Compos. Part A-Appl. S* **121** 418
[43] Xu W, Chen M, Lu X, Zhang D-W, Singh H-P, Jian-shu Y *et al* 2020 *Corros. Sci.* **168** 108557